Journal of Analytical and Applied Pyrolysis 164 (2022) 105542

Contents lists available at ScienceDirect

Journal of Analytical and Applied Pyrolysis

journal homepage: www.elsevier.com/locate/jaap

Effects of temperature and carrier gas on physico-chemical properties of biochar derived from biosolids

Shefali Aktar [a], Md Afzal Hossain [b], Nimesha Rathnayake [a], Savankumar Patel [a], Gabriel Gasco [c], Ana Mendez [d], Cicero de Figueiredo [e], Aravind Surapaneni [f], Kalpit Shah [a], Jorge Paz-Ferreiro [a,*]

[a] School of Engineering, RMIT University, Melbourne, Victoria 3000, Australia
[b] Department of Fisheries Management, Hajee Mohammad Danesh Science and Technology University, Dinajpur 5200, Bangladesh
[c] Department of Agricultural Production, Universidad Politécnica de Madrid, 28040 Madrid, Spain
[d] Department of Geological and Mining Engineering, Universidad Politécnica de Madrid, 28003 Madrid, Spain
[e] Faculty of Agronomy and Veterinary Medicine, University of Brasilia, 70910-970 Brasilia, DF, Brazil
[f] South East Water, 3199 Frankston, Victoria, Australia

ARTICLE INFO

Keywords:
Biosolids
Pyrolysis
Biochar
Temperature
Carrier gases

ABSTRACT

This study investigated the influence of temperature (400 °C, 500 °C and 600 °C) and –carrier gas (N_2 and CO_2) on biochar yields, physicochemical, and structural attributes. Higher temperatures resulted in less functional groups, higher surface area and lower H/C and O/C ratios. The biochar produced under N_2 environment was more alkaline and showed higher salinity whereas the biochar produced under CO_2 environment had higher surface area. The FTIR spectra of biochar produced in CO_2 atmosphere indicated the decrease of functional groups such as –OH, C═O, –CONH– and C═C with increasing pyrolysis temperature. However, the band intensity for Si–O–Si or Si–O–C and aromatic and hetero-aromatic structures were more prominent in biochar obtained in CO_2 environment than N_2 environment. The presence of calcium carbonate ($CaCO_3$), quartz (SiO_2) and magnesium calcite ($MgCO_3$) in biosolids and their biochars was confirmed by XRD spectrum. The outcomes from this research, particularly the stark contrast in biochar characteristics due to the variation in production conditions, inform the tailoring of biochars prepared under different conditions to environmental applications.

1. Introduction

Biosolids are treated sewage sludge generated during municipal wastewater treatment process. The global production rate of biosolids is rising due to the concomitant increase in human population and expansion of wastewater treatment facilities and has reached an amount of 371000 tonnes per year of dry solids in Australia in 2019 [1]. Typically, biosolids management have included land application, incineration and landfilling [2,3]. Largely, biosolids are applied to soils for agricultural purposes due to their inherent nutrient value. However, excess biosolids application may contaminate land through the release of pollutants such as heavy metals, pathogens and organic contaminants [4]. As a result, the land application of biosolids is under strict regulations in many countries, including Australia. Currently, water industries are faced with the challenge of managing biosolids around transportation costs, large biosolids volume and the presence of different organic and inorganic contaminants [5]. Thermochemical techniques such as pyrolysis, gasification and hydrothermal treatment are attractive for addressing these challenges and are under intense research exploration [6].

Pyrolysis is a widely investigated thermochemical method for converting biosolids to biochar under limited oxygen conditions. Pyrolysis can be categorised into fast and slow pyrolysis based on their residence time and heating rates. Slow pyrolysis maximises the yield of biochar and is typically used when the biochar is intended for use as soil amendment, due to the relatively mild operating conditions compared to fast pyrolysis [7,8]. Recently, the conversion of biosolids to biochar has attained a great interest because of easy destruction of pathogens and some organic contaminants while reducing waste volume and costs associated with biosolids transportation and stockpiling [2,9]. Biochar yield and attributes depend on pyrolysis conditions and feedstock characteristics [10]. Pyrolysis temperature is one of the most significant factors influencing yield and biochar physicochemical and structural properties. To a large extent, the influence of pyrolysis temperature on

* Corresponding author.
E-mail address: jorge.paz-ferreiro@rmit.edu.au (J. Paz-Ferreiro).

https://doi.org/10.1016/j.jaap.2022.105542
Received 7 November 2021; Received in revised form 21 March 2022; Accepted 28 April 2022
Available online 2 May 2022

biochar yield and properties is understood. For example, higher pyrolysis temperature lowers biochar yield and leads to a product with a larger number of aromatic carbon structures [11,12]. Many studies have demonstrated how biochar properties can be tailored to specific purposes, including increasing agro-environmental physicochemical properties, carbon sequestration or contaminant sorption, typically by controlling the production temperature [13,14]. The effect of carrier gas on the properties of biochar has been often overlooked, with most of the literature studying biochar production in a pyrolysis reactor under inert gas atmosphere usually N_2 [15]; or in muffle furnace under reduced oxygen environment [16]. The emission of CO_2 has increased continuously in the past decades due to human activities and it would be appealing to find novel uses to use this gas in industrial processes. Carbon dioxide could be used as a reaction medium in pyrolysis and this would alter the distribution and characteristics of the resulting fractions [17–19]. Studies comparing CO_2 and N_2 as a carrier gas in pyrolysis have predominantly focused on the production of bio-oil and pyrolysis gas [17,20,21] or in the determination of pyrolysis kinetic parameters [22,23]. The use of CO_2 as carrier gas with the purpose of altering the properties of the resulting biochars has not been systematically studied and information remains limited. Azuara et al. [24] reported similar stability for chars prepared under CO_2 or N_2 atmosphere. Using CO_2 atmosphere reduced the total and bioavailable polycyclic aromatic hydrocarbons (PAHs) [25] and resulted in higher surface area [18]. Replacing N_2 with CO_2 was found to increase total heavy metals contents in biochar; however, reducing the bioavailable fraction of the metals [26]. A reduction in the available heavy metals, particularly Pb, in soils amended with biochar was reported when using CO_2 compared to N_2 as carrier gas during biochar production [27]. However, there were no obvious differences in the microbial community in contaminated soils amended with biochar obtained under both atmospheres [28]. Finally, the kinetics of heavy metal release was significantly slower in biochar produced under CO_2 than in biochar produced under N_2 [27].

Given the extremely limited number of studies on the effect of carrier gas on biochar properties, there is a clear research gap on how these parameters influence a wide range of physico-chemical properties of biochars, in particular those of relevance for soil amendment. Therefore, the aim of our study was to obtain a detailed physicochemical characterisation of biochar produced from biosolids using three different temperature and two carrier gases. For this, we used a range of temperatures which have been commonly used to prepare biochar for soil amendment (400–600 ºC), avoiding to use higher temperatures, which have not shown agronomic advantages [29] and might result in the production of non-cost-effective biochars [30] or lower temperatures, which might result in phytotoxicity [31]. We hypothesise that, besides the control on biochar properties by the pyrolysis temperature, the use of a specific carrier gas would allow tailoring biochar for different applications.

2. Materials and methods

2.1. Biosolids collection

Biosolids were collected from Mount Martha Water recycle plant, Southeast water (38°16′06″ S and 145°03′31″ E), Melbourne, Australia. The raw sludge was treated by using lagoon and aerobic digester and the biosolids obtained are representative of other facilities in Australia and elsewhere. Then the sludge was processed by using sludge blend tank, dosing polymer and belt press. Moisture was reduced to 60% by solar dryers. Biosolids used in this experiment were collected from the solar dryer, grounded and sieved to 500–1000 μm particle size. Sampled biosolids were oven-dried at 105 °C for 24 hrs before pyrolysis.

2.2. Biochar preparation

Pyrolysis of biosolids was performed under slow pyrolysis mode in a fluidised bed reactor constructed of quartz tube, with internal diameter of 27 mm and height of 680 mm. This custom reactor was made by Monash scientific (Australia). Initially, 40 g of oven-dried biosolids were placed in the quartz tube reactor and introduced within the fluidised bed reactor before pyrolysis. The reactor was operated at atmospheric pressure and powered by energy from three electrical zones. Details of this reactor and the pyrolysis set up are described elsewhere [15]. Three different pyrolysis temperatures (400, 500 and 600 °C) were selected under nitrogen (N_2) and carbon dioxide (CO_2) atmospheres. The gas flow (N_2/ CO_2) was introduced to reactor and monitored by a mass flow controller (MFC). The set temperature reached with a standard heating rate of 35 °C/min and maintained for 60 min of heating under the carrier gas (N_2 / CO_2) sweeping at 7.5 L min^{-1}. The pyrolysis gas passed through steel condensers and caustic soda scrubber was used to remove any acid gas. The bio-oil was collected from the condenser and the gas was analysed online using a micro-GC / MRU. The solid product (biochar) was stored in a freezer. Biochar yield was calculated as the ratio of the weight of produced biochar to the dry weight of biosolids subjected to pyrolysis according to Eq. (1).

$$\text{Biochar yield } (\%) = 100^* \ (W_2/W_1) \quad (1)$$

where W_1 is the dry weight of biosolids sample before pyrolysis and W_2 is the weight of biochar. Biochar obtained were denoted as BN400, BN500, BN600 and BC400, BC500, BC600, where N and C represent the gas (N_2 and CO_2, respectively) and 400, 500 and 600 represent the maximum pyrolysis temperature. Biochar production at each condition was carried out three times and the average of the yields has been reported.

2.3. Determination of biochar physicochemical properties

2.3.1. Chemical analysis

Electrical conductivity (EC) and pH was measured in biosolids and their biochar by using 1 g sample added to 20 ml of deionized water and agitated for one hour on a mechanical shaker. The EC and pH were determined by using Five easy Mettler Toledo conductivity metre and pH metre respectively with results normalised to 25 °C [12]. The cation exchange capacity (CEC) of biosolids and biochar was measured by the ammonium acetate extraction methods. Briefly, 0.5 g biochar sample was measured in a volumetric flask, then, 20 ml of 1 M NH_4OAc (pH 7) was added and the mixture was stirred overnight. Finally, the solution was filtrated and 50 ml of 1 M NH_4OAc was added to leach Ca^{2+}, Mg^{2+}, K^+ and Na^+ which were measured in a Perkin Elmer 240 atomic absorption spectrophotometer [10].

2.3.2. Proximate and ultimate analysis

Thermogravimetric analysis (TGA) of biosolids and their biochar was performed in a Simultaneous Thermal Analyser (STA) 6000 (Perkin Elmer, USA). Perkin Elmer Software Pyris® was integrated with the instruments and this software was used for data collection and analysis. Initially, 2–10 mg of sample was heated from 35 °C to 105 °C at a rate of 10 °C/min and held for 3 mins at 105 °C. Then the sample was heated from 105° to 850°C under N_2 atmosphere at a flux of 20 ml/min. The pyrolysis gas was switched to air at 850 °C and the heating was continued until 900 °C at a rate of 10 °C and held for 5 mins at that temperature. The weight loss of the samples from 35° to 105°C was used to estimate the moisture content, while the major mass loss from 105° to 850°C was accrued to volatile matter (VM) content. The fixed carbon (FC) was determined by the mass loss in air atmosphere from 850° to 900°C. The final weight (%) after combustion at 900 °C was estimated as the ash content. Elemental Carbon (C), Hydrogen (H) and Nitrogen (N) were determined using CHNS/O analyser 2400 series II (PerkinElmer) via combustion at 950 °C. Samples (1.5–2.5 mg) were weighed using a Perkin-Elmer AD-4 ultra-microbalance. Total oxygen (O) was determined by difference as shown in Eq. (2).

Oxygen (O) (%w/w) = 100 − ash (%w/w) − C (%w/w) − H (%w/w) − N (%w/w) (2)

2.3.3. Fourier transform infrared spectroscopic (FTIR) analysis

FTIR spectroscopy analyses of biosolids and biochar were performed by using Perkin Elmer Spectrum 100 in the waveband of 4000–650 cm^{-1} scanned at a resolution of 4 cm^{-1}. The samples were powdered before use and the FTIR spectra were captured in absorbance mode.

2.3.4. Surface morphology and surface area

Surface images of the biosolids and their biochar were obtained using Philips XL30 Quanta 2 scanning electron microscope (SEM). The samples were loaded to the carbon tape on an aluminium stub treated with compressed air. Then, the loaded samples were coated with iridium using a vacuum sputter coating instrument. The thickness of coating was 5 nm. For comparing surface morphology, the SEM images were obtained at the same spot size (5.0) and magnification (x 1000). The surface area of biosolids and biochar were measured by using TriStar II 3020 gas adsorption BET analyser at 77k. Prior the analysis, around 200–300 mg of sample was degassed overnight under vacuum in a VacPrep™ 061 degasser at 180 °C for 24 h.

2.3.5. X-ray diffraction analysis (XRD)

Crystalline structure of biochar was measured by using X-ray diffractometer (XRD). The powdered biochar samples were loaded into an Al-holder tubes to identify the random powder XRD patterns. The XRD spectra was measured at an angle of 5–65 ° with a scan step size of 0.02 ° and time step of 1 s [12]. The peak areas identified for the different minerals were compared with XRD patterns of standard minerals compiled by the ICDD (International Centre Diffraction Data).

2.4. Statistical analysis of data

Data were tested for normality using Kolmogorov-Smirnov and Shapiro-Wilk test. Two-way analysis of variance (ANOVA) was performed to identify the significant effects of temperature, atmosphere and their interaction on biochar prepared at three different pyrolysis temperature and gas atmospheres. A post-hoc analyses was done for temperature using Tukey's test. All data are analysed using SPSS 26.0 version. Significance level was set at $P < 0.05$. The FTIR and XRD spectra were plotted by Origin 2016 and Spectrograph V1.2.14 software respectively.

3. Results and discussion

3.1. Influence of temperature and carrier gas on biochar yield

The yield of biochar produced at different pyrolysis temperatures is listed in Table 1. The yield gradually decreased with increasing pyrolysis temperature from 54% to 45% at 400–600 °C. The decrease in the yield at higher temperature is due to the decomposition of organic matter and polymerisation/condensation reactions increased with higher pyrolysis temperatures [12]. The biochar yield of 54.7% and 54.1% was similar at 400 °C under N_2 and CO_2 environment respectively. The results indicated that the carrier gas had a negligible impact on biochar yield at lower pyrolysis temperature. However, at higher pyrolysis temperatures, the yield of biochar was slightly reduced by ≈ 3 units at 500 °C under CO_2 atmosphere compared to N_2 atmosphere. CO_2 increased the thermal cracking efficiency of volatile compounds and had a profound decomposition of biomass organic macromolecules leading to lower char yield particularly at higher temperature [32,33]. This can be explained by three potential chemical effects of CO_2 on the yield of biomass biochar [19]. These are: (i) CO_2 might react with tar and inhibit secondary char formation (ii) CO_2 might directly react with the volatile compounds (iii) Due to Boudouard reaction (Eq. 3) where CO_2 may react directly with the char forming CO as a permanent gas. All the effects could directly or indirectly lower the biochar yield during pyrolysis using CO_2 as carrier gas.

$$C_{(s)} + CO_{2(g)} \rightleftarrows 2CO_{(g)} \quad (3)$$

However, at the highest temperature tested (600 °C), the yields of biochars prepared under both atmospheres were similar. This could be to the reverse Boudouard reaction being favoured at this range of temperatures. This effect was previously reported in feedstocks where Ni is present or, more generally, feedstocks with abundant inorganic matter [32].

3.2. Influence of pyrolysis condition on biochar properties

3.2.1. pH and electrical conductivity

The pH of the biochar produced from biosolids was influenced by pyrolysis temperature ($F = 80.14$, $P < 0.001$, Table 2). The pH (6.89) of biosolids was nearly neutral, while the biochar pH increased gradually from neutral to alkaline with increasing pyrolysis temperature from 7.30 at 400 °C to 9.45 at 600 °C (Table 1). The decline in acidic surface functional groups due to the decomposition of oxygen-containing

Table 1
Physicochemical properties of biosolids and their biochar obtained at different pyrolysis temperatures under N_2 and CO_2 atmospheres. Data were expressed as average ± S.E. .

Parameters		N_2 Environment			CO_2 Environment		
	Biosolids	BN400	BN500	BN600	BC400	BC500	BC600
Yield (%)		54.7 ± 0.3	50.3 ± 1.5	46.2 ± 0.1	54.1 ± 0.1	47.5 ± 0.5	46.2 ± 0.1
pH	6.89	7.47 ± 0.25	9.92 ± 0.30	11.26 ± 0.12	6.53 ± 0.23	7.34 ± 0.21	8.08 ± 0.05
EC (μS cm^{-1})	1084	72 ± 15	167 ± 14	406 ± 6	61 ± 1	131 ± 3	144 ± 14
C (%)	32.19	21.44 ± 0.54	16.29 ± 0.67	14.18 ± 0.43	20.64 ± 1.03	14.23 ± 0.45	13.24 ± 1.26
H (%)	4.45	1.68 ± 0.04	0.38 ± 0.07	0.23 ± 0.09	1.44 ± 0.09	0.27 ± 0.08	0.24 ± 0.09
N (%)	4.87	3.34 ± 0.03	2.63 ± 0.02	2.02 ± 0.06	3.19 ± 0.10	2.37 ± 0.05	2.09 ± 0.16
O (%)	27.73	20.43 ± 0.46	17.18 ± 0.31	18.48 ± 0.53	17.99 ± 1.15	21.25 ± 1.37	20.16 ± 1.41
H/C	1.65	0.94	0.17	0.32	0.83	0.23	0.21
C/N	7.71	7.48	7.23	8.19	7.55	7.01	7.39
O/C	0.65	0.72	0.82	0.98	0.65	1.12	1.14
CEC (cmol kg^{-1})	73.97	26.30 ± 1.33	34.73 ± 3.10	47.44 ± 2.89	28.48 ± 2.55	33.13.77 ± 2.06	36.55 ± 3.22
Moisture (%)	0.43	0.62 ± 0.18	0.80 ± 0.22	0.41 ± 0.22	1.08 ± 0.27	0.43 ± 0.17	0.67 ± o.17
VM (%)	53.63	22.78 ± 0.29	13.64 ± 0.34	10.23 ± 0.23	20.00 ± 0.71	13.59 ± 0.30	10.06 ± 0.19
FC (%)	15.17	22.48 ± 0.51	23.55 ± 0.80	24.28 ± 0.51	22.18 ± 0.71	24.09 ± 0.95	25.00 ± 0.05
Ash (%)	30.76	53.10 ± 0.35	62.99 ± 0.82	64.25 ± 0.57	55.73 ± 0.66	61.73 ± 1.01	64.27 ± 1.05
S_{BET} (m^2/g)	2.1	7.6	17.5	32.0	11.1	30.0	45.5
BJH Average pore volume (cm^3/g)	0.029	0.048	0.071	0.058	0.060	0.058	0.056
BJH Average Pore size (nm)	7.14	9.76	9.66	9.35	9.70	9.38	8.80

Table 2
Two-way analysis of variance (ANOVA) of physicochemical parameters of biochar obtained at different pyrolysis temperatures under N_2 and CO_2atmospheres. Significance was set at $P < 0.05$.

Source	Variable	df	Mean square	F	*P*
Environment	Moisture	1	0.06	0.47	0.51
	VM	1	4.56	10.37	**0.01**
	FC	1	0.47	0.36	0.56
	Ash	1	1.71	1.32	0.27
	pH	1	22.47	165.82	**<0.001**
	EC	1	27,524.05	103.66	**<0.001**
	CEC	1	58.03	9.73	**0.01**
	C	1	7.18	3.80	0.08
	H	1	0.06	3.20	0.10
	N	1	0.06	2.85	0.12
	O	1	3.47	1.20	0.29
Temperature	Moisture	2	0.16	1.27	0.32
	VM	**2**	**198.58**	**451.76**	**<0.001**
	FC	**2**	**5.26**	**4.10**	**0.04**
	Ash	**2**	**154.77**	**119.82**	**<0.001**
	pH	**2**	**10.86**	**80.14**	**<0.001**
	EC	**2**	**81,114.36**	**305.49**	**<0.001**
	CEC	**2**	**311.37**	**52.21**	**<0.001**
	C	**2**	**89.42**	**47.25**	**<0.001**
	H	**2**	**3.30**	**175.75**	**<0.001**
	N	**2**	**2.25**	**106.75**	**<0.001**
	O	2	0.19	0.07	0.94
Environment	Moisture	2	0.28	2.20	0.15
× Temperature	VM	**2**	**3.58**	**8.15**	**0.01**
	FC	2	3.23	2.52	0.12
	Ash	**2**	**10.27**	**7.95**	**0.01**
	pH	**2**	**2.00**	**14.75**	**<0.001**
	EC	**2**	**31,112.18**	**117.17**	**<0.001**
	CEC	**2**	**64.01**	**10.73**	**<0.001**
	C	2	0.71	0.37	0.70
	H	2	0.03	1.62	0.24
	N	2	0.04	2.03	0.17
	O	**2**	**13.41**	**4.64**	**0.03**

chemical groups could explain the slight alkaline pH of the biochar at high temperature. This result was confirmed by the FTIR spectra (Fig. 1A & 1B), which showed a weaker band intensity for acidic surface functional group for 3400 cm^{-1}, 2923 cm^{-1} and 1220 cm^{-1} with increasing pyrolysis temperature. Also, the increase in the concentration of alkali and alkaline earth metal salts including the formation of carbonates in the biochar at higher temperature led to the gradual change of pH from neutral to alkaline [13,34].

The pH of the biochar was significantly affected by the carrier gas ($P < 0.001$, $F = 165.82$, Table 2). Biochar pH values were about 2 units higher when using N_2 compared to CO_2. The elevated biochar alkalinity in N_2 atmosphere has been ascribed to the transformation of nitrogen-containing functional groups like pyrimidine from amine alongside the decrease of acidic surface functional groups [35]. The weaker band intensity at 3400 cm^{-1} for -OH groups under CO_2 than that in N_2, indicating CO promotes the rupture of hydroxyl groups regardless of the temperatures. The decomposed hydroxyl groups would transfer to phenols, water, and CO. Moreover, the presence of more acidic oxides (such as V_2O_5) and lower content of magnesium calcite confirmed by XRD (Table 3) may contribute to the decrease in biochar pH produced under CO_2 compared to N_2 environment. Additionally, the strong peak at 1035 cm^{-1} assigned to Si–O–Si or S–O–C structures which acts as weakly acidic molecules was more intense under CO_2 than under N_2 atmosphere. Biochar prepared under CO_2 environment had more ketones and acidic groups at higher temperature explaining the slightly acidic to neutral pH of the biochar in CO_2 media compared to the N_2 [18].

There was a significant interaction between temperature and carrier gas on the biochar pH ($P < 0.001$, $F = 14.75$, Table 2). The increase in biochar pH with pyrolysis temperature was observed to occur at a quicker pace under N_2 environment than the CO_2 environment (Table 1). For instance, biochar pH increased by 2.5 units from 400 °C to 500 °C under N_2 atmosphere, while it increased by 0.8 units under CO_2 at the same temperature range. Electrical conductivity (EC) indicates the amount of soluble salt presents in the samples. The highest EC (1084 μS cm^{-1}, Table 1) was observed in biosolids and it was greatly reduced in the biochar to 72 μS cm^{-1} in BN400 and 61 μS cm^{-1} in BC400. However, the EC value increased with increasing pyrolysis temperatures reaching to 406 μS cm^{-1} in BN600 and 144 μS cm^{-1} in BC600. EC content in the biochar were significantly influenced by temperature ($P < 0.001$, $F = 305.49$, Table 2). The increasing pyrolysis temperature was associated with the loss of volatile materials, which will be reduced the element concentration in ash fraction [36,37]. Biochar produced under CO_2 showed lower (approximately 100 μS cm^{-1}) EC than biochar produced using N_2 environment ($P < 0.001$, $F = 103.66$, Table 2). Lower values of EC in biochars prepared under CO_2 could be related to the amount of salts (calcite, iron phosphate hydroxide and magnesium calcite) being lower in biochars produced under CO_2 compared to those produced under N_2 atmosphere. There was a significant interaction between temperature and carrier gas ($P < 0.001$, $F = 117.17$, Table 2) on the biochar EC. For example, biochar EC increased by 5 times from a temperature of 400 °C to 600 °C under N_2 atmosphere, while it increased by 2 times under CO_2 at the same temperature range.

3.2.2. Cation exchange capacity

Biosolids had the highest CEC (73.97 cmol kg^{-1}) compared to the biochars (Table 1). Cation exchange capacity (CEC) of the biochar was significantly affected by pyrolysis temperature ($P < 0.001$, $F = 52.21$, Table 2). Biochar CEC gradually increased from 26.30 cmol kg^{-1} at 400 °C to 47.44 cmol kg^{-1} at 600 °C under N_2 environment. A similar CEC increment was also observed in biochar under CO_2 environment from 28.48 cmol kg^{-1} at 400 °C to 36.55 cmol kg^{-1} at 600 °C. The reduction in CEC in the biochar compared to biosolids could be due to the removal of surface functional groups and the formation of aromatic carbon [38]. Biochar CEC is controlled by the nature and distribution of O-containing functional groups on the biochar surface. The negative surface charge comes from carboxylate (COO^-) groups and phenolate (Ph-O^-) groups, while oxonium groups (O^+ heteroatoms in aromatic rings) provides only positive charge [39]. Therefore, biochar with higher CEC is mainly found due to the surface functional group with anionic effects that includes ester (-C(=O)OR), aldehydes (-C(=O)H), carboxyl (-COOH), ketone (-C═O)R), hydroxyl (-OH), and amino ($-NH_2$) during pyrolysis [40]. This was confirmed by the stronger band intensity at 1000–1800 cm^{-1} indicating the abundance of oxygen containing functional groups (-OH and C-O) with increasing pyrolysis temperature. However, under acidic condition, the π electrons of condensed aromatic structures are able to abstract protons from solutions [39]. CEC was influenced by the pyrolysis carrier gas ($P => 0.010$, $F = 9.73$, Table 2). There was a significant interaction between temperature and carrier gas ($P < 0.001$, $F = 10.73$, Table 2) on the biochar CEC.

3.2.3. Elemental composition

The elemental (C, H and N) contents in the biochar substantially decreased with increasing pyrolysis temperature. Carbon (C) content decreased with temperature ($P < 0.001$, $F = 47.25$, Table 2) from 21% at 400 °C to 14% at 600 °C (Table 1). The C content decreased noticeably with increasing pyrolysis temperature in biochar, similarly to other studies [12,41]. The decreased C concentration with increasing temperature was due to dehydration and decarboxylation reactions where the light organic compounds are transformed into volatile materials in the forms of CO, CO_2, H_2O and hydrocarbons during the pyrolysis process [17,42]. Compared to other feedstocks, the carbon fractions of biosolids are more vulnerable to thermal decomposition [43]. The reduced band intensity related to C-H aliphatic groups was confirmed by the FTIR spectra with increasing pyrolysis temperature under both atmosphere (N_2 and CO_2). Pyrolysis environment ($P = 0.08$, $F = 3.80$, Table 2) did not have a significant effect on C and there was no

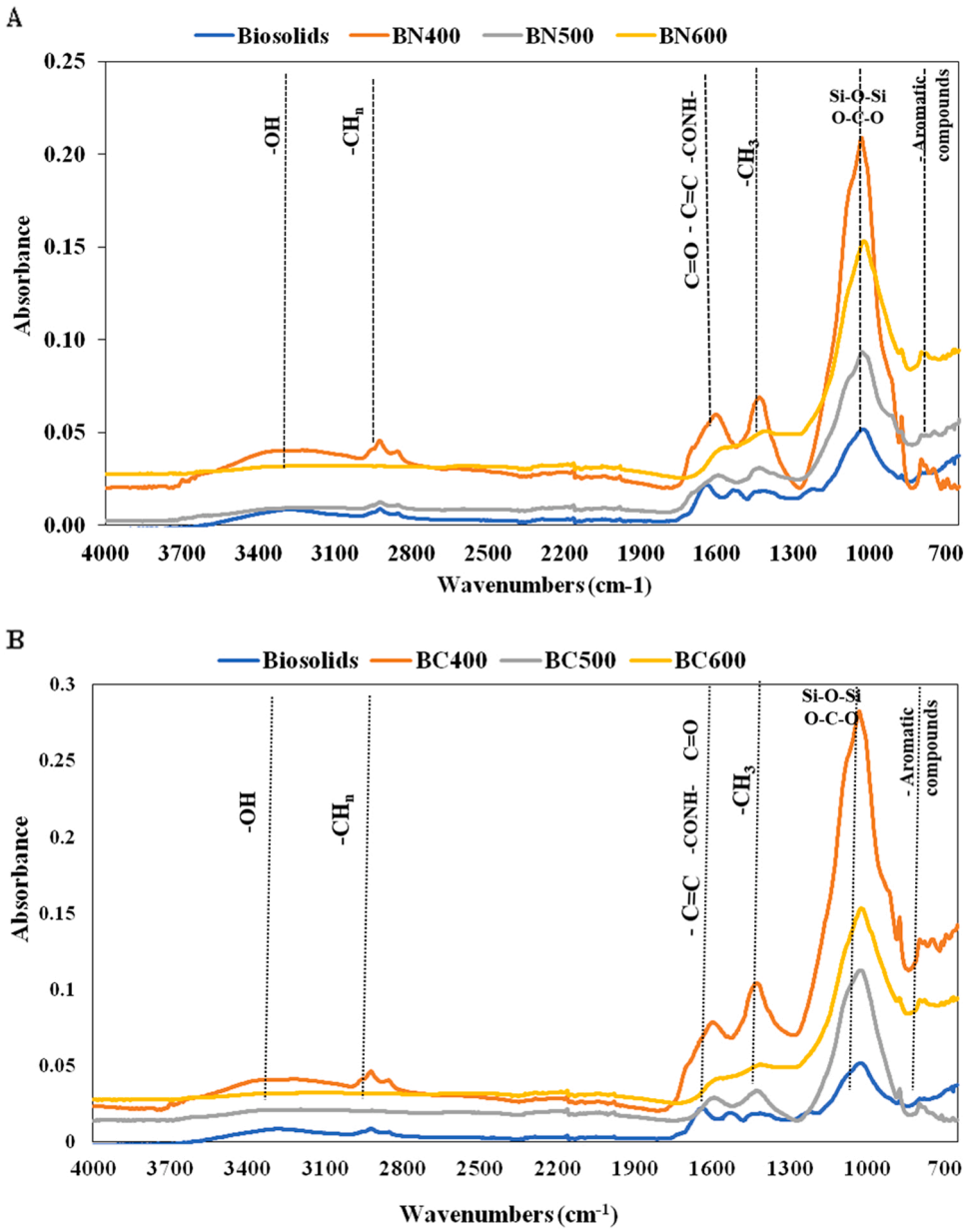

Fig. 1. FTIR spectra of biosolids and their biochar at different temperatures under N_2 atmosphere A) and CO_2 atmosphere (B).

significant interaction between the temperature and environment ($P = 0.70$, $F = 0.37$, Table 2).

Similarly, hydrogen (H) and nitrogen (N) concentrations decreased with increasing pyrolysis temperature (For H: F = 175.75, N: F = 106.75, $P < 0.001$ Table 2). The biochar H contents was highest 1.68% at 400 ºC and decreased to 0.24% at 600 ºC (Table 1). The total content of H decreased gradually with increasing pyrolysis temperature under both environments. The increase in the biochar aromaticity due to the combination or elimination of -OH, $-CH_3$, $-CH_2$, and -C═O at higher temperature caused the decline in H contents [44]. Similarly, the N concentration decreased from 3.27% at 400 ºC to 2.06% at 600 ºC. This may be attributed to the decomposition of N-containing compounds (N_2O, NO, and NO_2) [45] and transformation into heterocyclic aromatic form with more stable structures (for example pyridine, pyrrole, and quaternary nitrogen).

Both H and N contents were not statistically influenced by carrier gas ($P \geq 0.10$, Table 2) and the interaction between temperature and carrier gas was not significant ($P = 0.24$, Table 2).

The decrease in molar H/C ratio indicated an increase in aromaticity due to strong carbonisation in the biochar with increasing pyrolysis temperature. BN500 had the lowest H/C molar ratio (0.17) compared to 0.94 for BN400 and 0.32 for BN600 (Table 1). However, when CO_2 was used as carrier gas, BC600 had the lowest H/C (highest aromaticity) at 0.21 compared to 0.83 for BC400 and 0.23 for BC500. The O/C ratio increased by 1.5 times in CO_2 compared to N_2 environment. The molar O/C ratio is related to oxygen functional groups and its surface hydrophilicity of carbon materials. The O/C was slightly higher (BC400: 0.65 & BC600:1.14) under CO_2 with increasing pyrolysis temperature compared to N_2 (BN400: 0.72 & BN600:0.98). The decrease of H/C was related to the increased in aromatisation and carbonisation reaction in biochar produced at 600 ºC under CO_2 atmosphere and while the O/C suggested that the biochar produced exhibited higher hydrophilic characteristics at 600 ºC as it has a much higher O/C ratio [46] characteristics than those produced under N_2 atmosphere, similar to the observations made in earlier studies [18,46].

3.2.4. *Functional groups distribution*

The FTIR analysis of biosolids and their biochar at three different

Table 3
Identification of different mineral phases in biosolids and their biochars.

	N_2						CO_2					
	BN400		BN500		BN600		BC400		BC500		BC600	
Compound	(%)	Compound	(%)	Compound	(%)	Compound	(%)	Compound	(%)	Compound	(%)	Compound	(%)
Quartz (Q) (SiO_2)	18.7	Quartz (Q) (SiO_2)	12.3	Quartz (Q) (SiO_2)	38.2	Quartz (Q) (SiO_2)	26.2	Quartz (Q) (SiO_2)	18.6	Quartz (Q) (SiO_2)	10.7	Quartz (Q) (SiO_2)	30.0
Calcite(C) $CaCO_3$	13.4	Calcite(C) $CaCO_3$	7.3	Calcite(C) $CaCO_3$	20.2	Calcite(C) $CaCO_3$	12.1	Calcite(C) $CaCO_3$	13.4	Calcite(C) $CaCO_3$	5.9	Calcite(C) $CaCO_3$	20.1
Aluminium phosphate (AP) $AlPO_4$	3.4	Aluminium phosphate (AP) $AlPO_4$	4.0	Aluminium phosphate (AP) $AlPO_4$	6.8	Aluminium phosphate (AP) $AlPO_4$	5.5	Aluminium phosphate (AP) $AlPO_4$	9.6	Aluminium phosphate (AP) $AlPO_4$	1.1	Aluminium Phosphate (AP) $AlPO_4$	6.1
Magnesium calcite (MC) MgO.03CaO.97 (CO_3)	9.6	Magnesium calcite (MC) MgO.03CaO.97 (CO_3)	8.3	Magnesium calcite (MC) MgO.03CaO.97 (CO_3)	15.1	Magnesium calcite (MC) MgO.03CaO.97 (CO_3)	10.1	Magnesium calcite (MC) MgO.03CaO.97 (CO_3)	9.5	Magnesium calcite (MC) MgO.03CaO.97 (CO_3)	7.1	Magnesium calcite (MC) MgO.03CaO.97 (CO_3)	6.2
Iron vanadium oxide (IVO) (Fe6.5V11.5O35)	21.2	Iron vanadium oxide (IVO) (Fe6.5V11.5O35)	25.7	Iron vanadium oxide (IVO) (Fe6.5V11.5O35)	5.5	Iron vanadium oxide (IVO) (Fe6.5V11.5O35)	28.0	Iron vanadium oxide (IVO) (Fe6.5V11.5O35)	23.8	Iron vanadium oxide (IVO) (Fe6.5V11.5O35)	26.2	Iron vanadium oxide (IVO) (Fe6.5V11.5O35)	14.6
Iron phosphate hydroxide (IPH) Fe $(PO_4)_3(OH)_3$	24.2	Iron phosphate hydroxide (IPH) Fe $(PO_4)_3(OH)_3$	13.5	Iron phosphate hydroxide (IPH) Fe $(PO_4)_3(OH)_3$	5.4	Iron phosphate hydroxide (IPH) Fe $(PO_4)_3(OH)_3$	7.9	Iron phosphate hydroxide (IPH) Fe $(PO_4)_3(OH)_3$	20.9	Iron phosphate hydroxide (IPH) Fe $(PO_4)_3(OH)_3$	19.8	Iron Phosphate hydroxide (IPH) Fe $(PO_4)_3(OH)_3$	18.0
Zinc phosphate (ZP) $Zn_2P_2O_7$	9.5	Zinc phosphate (ZP) $Zn_2P_2O_7$	28.9	Zinc phosphate (ZP) $Zn_2P_2O_7$	8.8	Zinc phosphate (ZP) $Zn_2P_2O_7$	10.1	Zinc phosphate (ZP) $Zn_2P_2O_7$	4.3	Zinc phosphate (ZP) $Zn_2P_2O_7$	19.0	Zinc phosphate (ZP) $Zn_2P_2O_7$	5.0

temperatures under N_2 and CO_2 atmosphere are shown in Fig. 1. A and Fig. 1. B, respectively. Overall, the results showed that the major functional groups in the biosolids disappeared in the biochar after pyrolysis, especially above 400 °C. The strong-band intensity of the band at around 3400–3700 cm^{-1} was attributed to hydroxyl functionalities (the stretching vibration of -OH), which decreased rapidly with increasing pyrolysis temperature. This result indicated that a large amount of free, associated hydroxyl and structural hydroxyl groups (-COOH and -COH) were decomposed during biosolids pyrolysis with increasing temperature [47]. Meanwhile, the bands absorbance in biosolids at 2800–2922 cm^{-1} assigned to aliphatic CH_n groups (C-H stretching) reduced considerably at higher pyrolysis temperature ($\geq$ 500 °C) in biochar under N_2 (Fig. 1. A), while the band intensity totally disappeared in biochar produced under CO_2 (Fig. 1. B). Comparing between two carrier gases, it was observed that most of the biochar chemical components in the spectra between 3285 and 2853 cm^{-1} in CO_2 atmosphere disappeared or remarkably attenuated than those in biochar produced under N_2 atmosphere. Notably the use of CO_2 gas had a positive impact on the removal of -CH stretching in methylene group and the organic fatty hydrocarbons were transformed into aromatic structures by producing CO_2, CH_4, and other gases [48,49]. The intense band at around 1642–1537 cm^{-1} were sharper (Fig. 1. A) under N_2 environment compared to CO_2 atmosphere (Fig. 1. B). This band represents the amide bonds and/or aromatic ring stretching (C═O and C═C stretching vibration) and reduced slightly with increasing pyrolysis temperature from 400 °C to 600 °C. The band at around 1550 cm^{-1} was mainly due to the presence of asymmetric stretching of carboxylate groups [50].

The 1418–435 cm^{-1} band represents (CH_3 and CH_2 groups) typical of C═C bond of aromatic rings polarised by oxygen atoms bound near one of the C atoms suggesting the presence of basic oxygen containing functional group such as pyrone group or diketones [20]. The band was slightly decreased in biochar under CO_2 environment, indicating less aliphatic and cycloalkane structures, than the N_2 environment with increasing pyrolysis temperature [51]. The strong band at 1035 cm^{-1} can be related to Si–O–Si or Si–O–C structures which exhibited only a sharp change in biochar at 400 °C pyrolysis temperature under CO_2 environment. This is likely associated by silicon oxide present in biosolids and biochar [52]. The intensity of bands at 1000–1800 cm^{-1} mainly indicated the abundance information about oxygen containing functional groups and the C═C suggesting that the biochar produced under CO_2 atmosphere had more content of C═C, -OH, and C-O immobilised in the char compared to N_2 environment [53]. The low-intensity bands between 795 cm^{-1} and 897 cm^{-1} was assigned to aromatic groups and hetero-aromatic compounds and had sharper intensity in CO_2 environment [14]. The band intensity at 875–715 cm^{-1} represents $CaCO_3$ Jin et al. [54], aromatic and heteroaromatic compounds [14,51] which increased with pyrolysis temperature under both atmospheres. The presence of $CaCO_3$ and quartz (SiO_2) in biosolids and biochar was confirmed by the XRD spectra (Fig. 4). The higher intensity band of aromatic bending in CO_2 than in N_2 implied that the formation of polycondensation was higher during CO_2 pyrolysis [53]. The aromatic groups can provide π-electrons which have been found to have the potential to bond strongly with heavy metal cations [55]. There was metal halogen stretching vibrations in both organic and inorganic halogen compounds in bands below 600 cm^{-1} in all biochar spectra [14].

3.2.5. Proximate analysis

Thermal analysis of biochar produced from biosolids showed that temperature had a statistically significant effects on ash content ($P < 0.001, F = 119.82$, Table 2) and on volatile matter ($P < 0.001, F = 451.76$, Table 2). Ash content of biochar gradually increased with temperature from 54.92% at 400 °C to 64.60% at 500 °C. Volatile matter (VM) exhibited opposite trend; it decreased with increasing pyrolysis temperature (Table 1). Fixed carbon (FC) gradually increased with pyrolysis temperature from 22.83% at 400 °C to 24.64% at 600 °C. The

increasing ash content with pyrolysis temperature was due to the decomposition of organic matter and formation of ash from either non-volatile mineral constituents or with the removal of volatile organic decomposition products [56]. The labile carbon in VM can get converted into stable form at high pyrolysis temperature thereby increasing the FC contents [16]. Pyrolysis environment had no significant effect on the biochar ash and fixed carbon contents ($P = 0.27$), whereas the VM was significantly affected by the carrier gas environment ($P < 0.001$, $F = 10.37$, Table 2). The interactive effects of pyrolysis temperature and environment was significant on biochar ash content ($P < 0.001$). Ash content was increased with temperature at a quicker pace under N_2. For example, biochar ash increased by 10 units from 400 °C to 500 °C under N_2 atmosphere, while it increased by 8 units under CO_2 at the same temperature interval. The content of ash, volatile matter and fixed carbon in biochar impacts its environmental application. Biochars with higher fixed carbon content in biochar are chemically and biologically stable, having half-lives in soil over 100–1000 years [57].

3.3. Morphological study of biochar

The morphological study of biosolids showed a smooth surface with limited porous structure, while biochar had rough surface with well-developed pores (Fig. 2). The porous structure of biochar developed gradually with increasing pyrolysis temperature. BN400 showed some well-developed porous structure in SEM image under N_2 environment (Fig. 2). The development of pores was advanced in BN500 and a crack of pore surface can be seen in BN600. Similarly, in comparison of SEM images, BC400 showed well-developed porous structure, holes formation occurred in BC500, and the number of holes were reduced in BC600. The current development of porous structure in biochar under CO_2 atmosphere was probably resulted from the destruction of biochar structure, hence weakened the interaction between H and the biochar matrix. This property can increase the formation of biochar with high porosity and high specific surface area [18].

The BET specific surface area of biochar produced are presented in

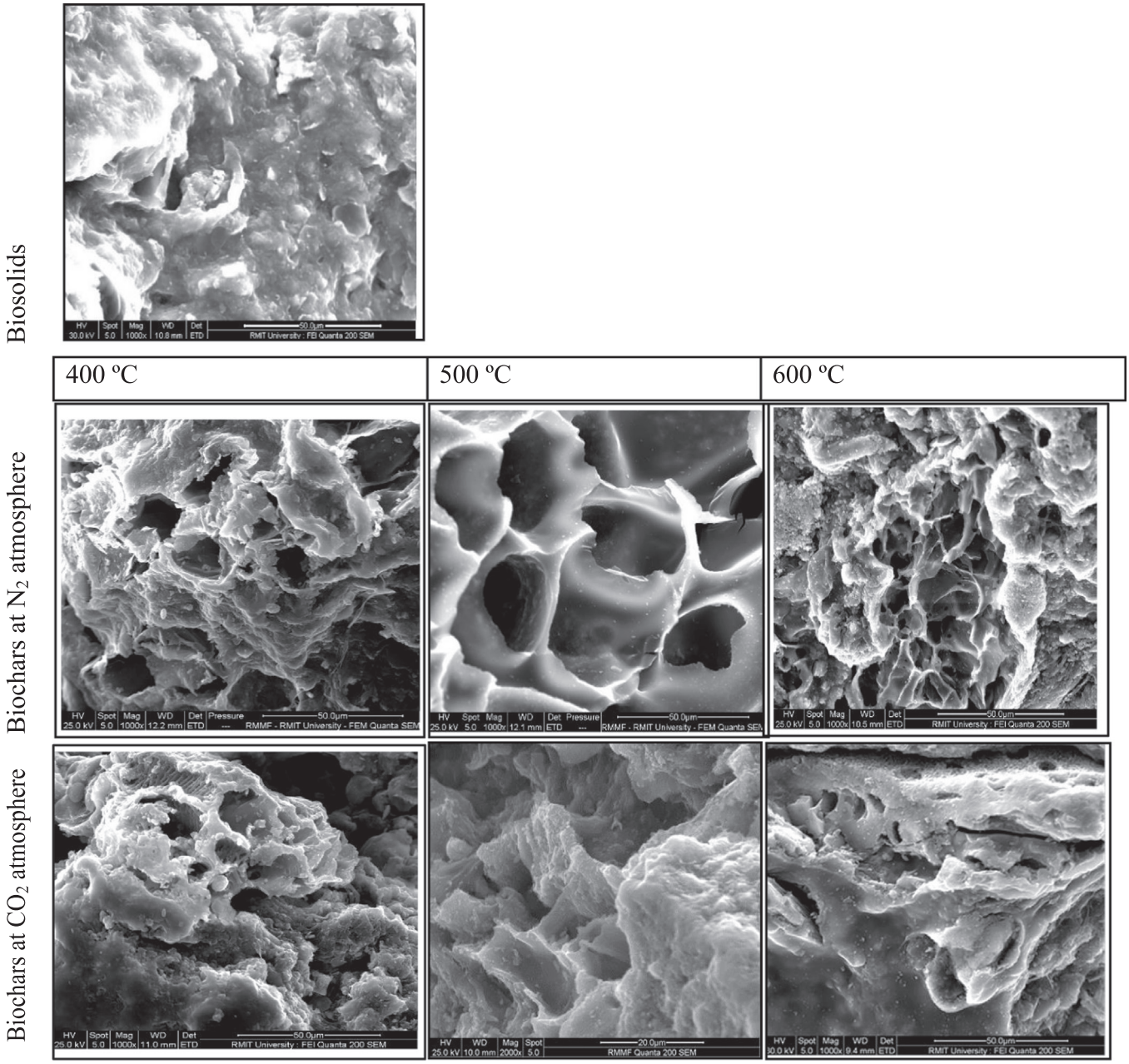

Fig. 2. SEM images of biosolids and biochar at three different temperatures (400, 500 and 600 °C) under two atmospheres (N_2 and CO_2).

Table 1. The original feedstock had a very low surface area (2.1 m^2/g). The BET surface area (S_{BET}) of biochar increased from 7.6 m^2/g at 400 °C to 32.0 m^2/g at 600 °C under N_2 environment. Pyrolysis under CO2 leads to higher surface areas, with values from 11.4 m^2/g at 400 °C to 45.5 m^2/g at 600 °C. Previous studies [12,13,16] reported a higher S_{BET} value for biochar from biosolids than the ones obtained in the current study. The increase in surface area with increasing pyrolysis temperature could be associated with the removal of VM that creates more mesopore and micropore at higher pyrolysis temperature. However, the surface area increased significantly from 11.4 m^2/g (BC400) to 45.5 m^2/g (BC600) under CO_2 environment due to effects of CO_2 gasification. Jindarom et al. [58] reported that CO_2 gasification removed carbon atoms from the interior of biomass particles. As a result, the open micropores were enlarged and enhanced the opening of closed micropores. It was observed that the biochar produced under CO_2 environment showed higher N_2 adsorption/desorption isotherm curves (Fig. 3 (B)) than the biochar under N_2 (Fig. 3. A). The pore size of biochar can be divided into micropores (internal pore diameter <2 nm) which is responsible for high adsorption capacity for small molecules such as gas and common solvents; mesopores (internal pore width, 2–50 nm) and macropores (pore of internal diameter >50 nm) [59]. As shown in the Table 1, all the biochars were mesoporous. The pore size distribution showed that biochar produced at 400 °C have higher pore size 9.757 nm for BN400 and 9.701 nm for BC400. The pore size decreased gradually in biochar produced at higher temperature in both environments. The results demonstrated that the pore size might collapse at higher temperature, resulting in a decrease in pore size [60].

3.4. Crystalline structure of biochar

The crystalline phase of biosolids derived biochar was identified by XRD analysis. Quartz (SiO_2) with a characteristic peak at $2\theta = 26.6°$ was commonly identified crystalline structure in the biosolids and the resulted biochar (Fig. 4). Biochar obtained from biosolids contains higher amount of silica when prepared at high temperatures peak intensity, possibly due to the change in ultrastructure of sludge biochar. The percentage of silica content (Table 3) in the biochar (12.3.9 to 38.2%) was similar to results reported by [18]. Calcite ($CaCO_3$) was the next crystalline phase that was identified in substantial quantity in both biosolids and their biochar under both atmospheres. Liu et al. [61] reported that $CaCO_3$ and SiO_2 may participate in the immobilisation of Zn, Pb and Cr at high pyrolysis temperature. There was some background noise attributed to organic matter vibration in the samples. $CaCO_3$ and magnesium calcite ($MgO.CaCO_3$) appeared in diffraction peak at 2θ value of 29.44–49.51 and their intensity increased with increasing pyrolysis temperature, particularly for calcite [62]. In general, the mineralogical composition of the biochar was not affected by the pyrolysis environment. The common major mineral bearing elements are calcium, iron, aluminium and phosphorus with calcite, magnesium calcite, iron phosphate hydroxide, aluminium phosphate, calcium magnesium phosphate, zinc phosphate and iron vanadium oxide being the major mineral species in all biochars (Table 3).

3.5. Implications of our research

The current paradigm in biochar use for soil amendment establishes that there are trade-offs for different potential benefits of soil application, for example, when using biochar with the intention to maximise carbon sequestration, which corresponds to biochars prepared at high temperatures, there could be a decrease in its potential for increasing soil fertility [63]. Our study has confirmed some trends found before, for example, higher pH, EC, fixed carbon content and surface area as the temperature of pyrolysis increases [2]. Importantly, it has been demonstrated that biochars prepared under carbon dioxide have intrinsically different physico-chemical characteristics to those prepared under nitrogen. Biochars prepared under carbon dioxide were much less alkaline than those prepared under nitrogen and exhibited a lower EC. This could be of importance in calcareous soils, where the agricultural benefits of biochar application have demonstrated to date to be limited [64] and high salinity limit crop productivity. In addition, higher surface areas, together with a shift in functional groups, were found in biochars prepared under carbon dioxide, which would have implications for the sorption of contaminants, both in aqueous and terrestrial environments. The use of CO_2 instead of N_2 as pyrolysis atmosphere led to similar or better results concerning properties involved in soil carbon sequestration (H/C, O/C ratios and fixed carbon). Overall, some advantageous properties when using carbon dioxide as pyrolysis atmosphere were identified. Although not a focus in this study, it was previously found that using CO_2 as pyrolysis atmosphere can decrease the bioavailability of PAHs [25] and heavy metals [65]. Future research should focus in finding specific opportunities to maximise the potential environmental benefits of biochars prepared under carbon dioxide.

4. Conclusions

The pyrolytic conversion of biosolids to biochar at different temperatures under two carrier gas offered a simple method for tailoring biochar properties to different environmental applications. The pyrolysis temperatures and atmospheres influenced the biochar yield as well as several physicochemical and structural attributes of the biochar. Increasing pyrolysis temperature from 400 °C to 600 °C reduced the biochar yield but increased the biochar aromatic structures, reduced the

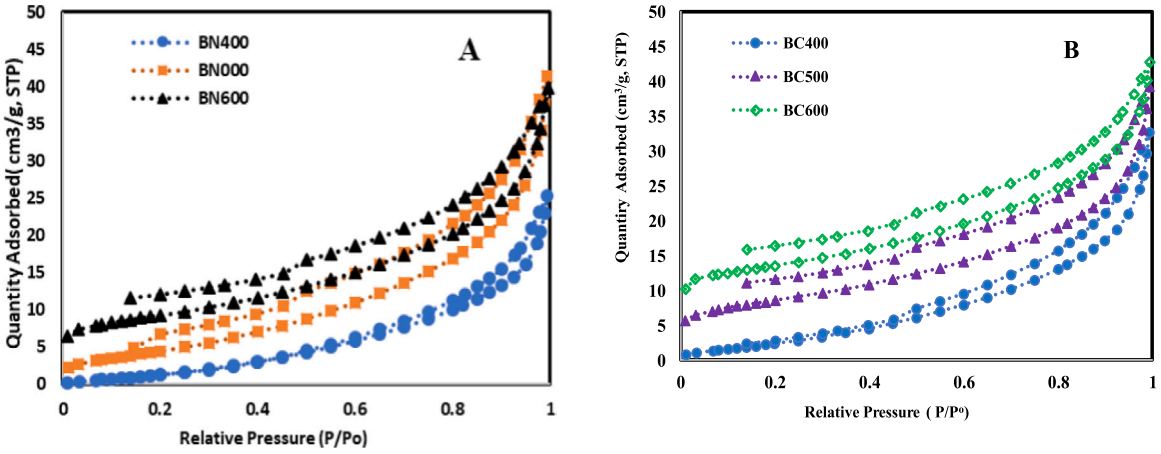

Fig. 3. N_2 adsorption/desorption isotherm report for biochar produced at three different temperatures under (A) Biochar produced under N_2 and (B) Biochar produced under CO_2 atmosphere.

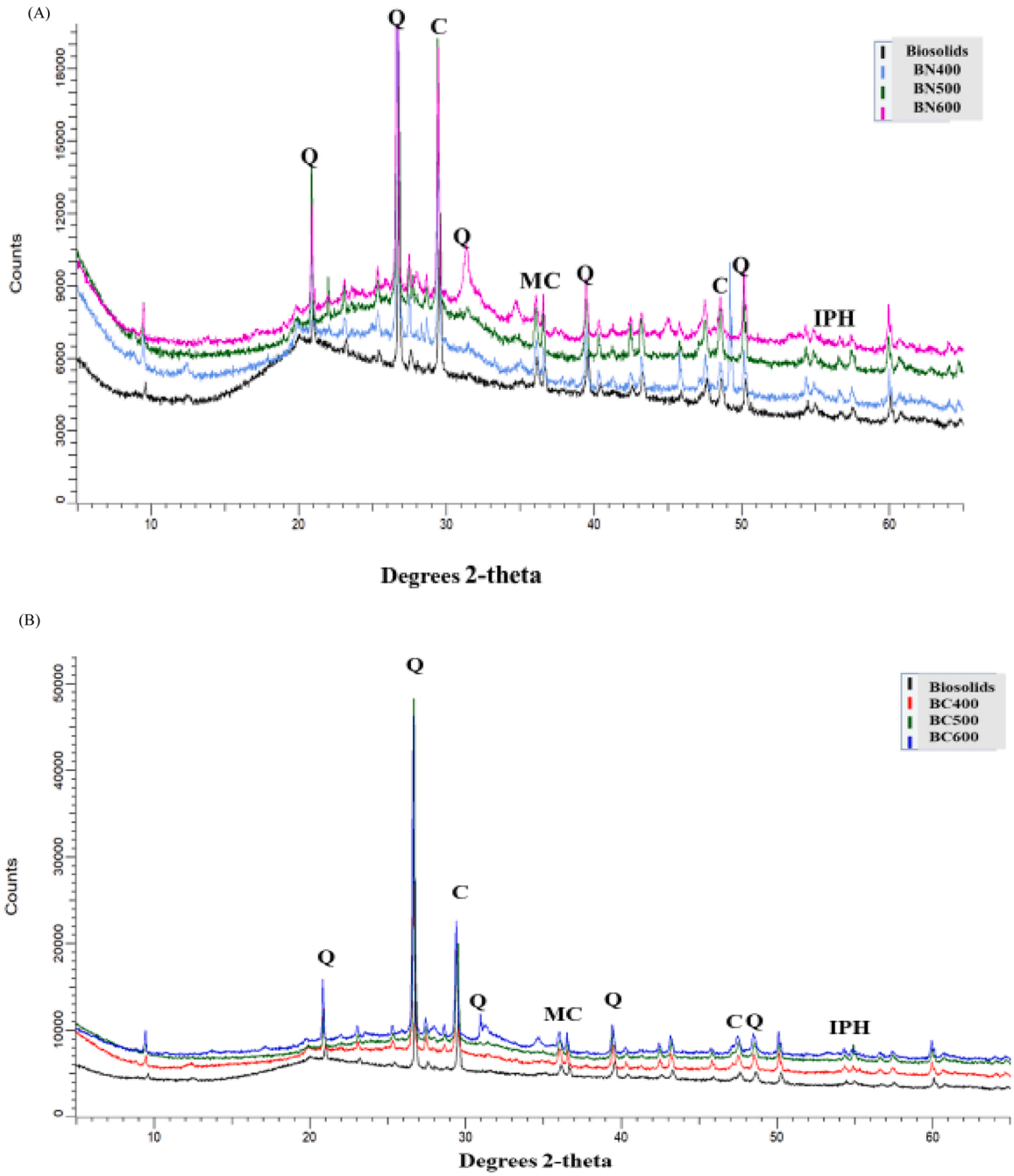

Fig. 4. XRD spectra of biosolids and biochars at different temperature under N_2 (A) and CO_2 (B) atmosphere, where (Q) Quartz, (C) Calcite, (MC) Magnesium calcite ($MgO.CaCO_3$), (IPH) Iron Phosphate hydroxide Fe $(PO_4)_3(OH)$.

surface functional groups and increased the pH. Replacing an expensive inert gas (N_2) with carbon dioxide is of interest as it reduces operating costs and results in a similar yield of biochar with some similar physico-chemical properties (particularly those involved in soil carbon sequestration) and better porosity. Notably, biochar pH, a property fundamental for soil remediation, particularly for heavy metals immobilisation and for soil fertility as it modulates nutrient availability, was significantly different when using CO_2 as a carrier gas. Thus, biochars prepared under different atmospheres will exhibit a contrasting behaviour when added to the soil. The next stage of this research would be to find niche areas where biochars prepared from carbon dioxide could outperform other type of biochars.

CRediT authorship contribution statement

Shefali Aktar: Conceptualization, Writing – original draft, Data curation, Investigation. **Md Afzal Hossain:** Conceptualization, Writing – review & editing. **Nimesha Ratnnayake:** Conceptualization, Writing – review & editing. **Savankumar Patel:** Conceptualization, Writing – review & editing, **Gabriel Gasco:** Conceptualization, Writing – review & editing. **Ana Mendez:** Conceptualization, Writing – review & editing. **Cicero de Figueiredo:** Conceptualization, Writing – review & editing. **Aravind Surapaneni:** Conceptualization, Writing – review & editing. **Kalpit Shah:** Conceptualization, Supervision, Writing – review & editing. **Jorge Paz-Ferreiro:** Conceptualization, Supervision, Writing – review & editing.

Declaration of Competing Interest

The authors declare that they have no known competing financial interests or personal relationships that could have appeared to influence the work reported in this paper.

Acknowledgement

The first author would like to acknowledge the School of Engineering, RMIT University for providing a Ph.D. scholarship and associated research funds. We appreciate the support from RMIT Microscopy and Microanalysis Facility (RMMF) in the SEM analyses for this work. We also acknowledge Professor Rachel A. Caruso, ECP Director, Advanced Materials Research & Innovation Capability for providing the opportunity to use the BET instrument.

References

[1] ANZBP, Australian Biosolids Statistics. Australian Water Association, 2019. ⟨https://www.biosolids.com.au/guidelines/australian-biosolids-statistics⟩.
[2] J. Paz-Ferreiro, A. Nieto, A. Méndez, M.P.J. Askeland, G. Gascó, Biochar from biosolids pyrolysis: a review, Int. J. Environ. Res. Public Health 15 (2018) 956.
[3] R.J. LeBlanc, P. Matthews, R.P. Richard, Global atlas of excreta, wastewater sludge, and biosolids management: moving forward the sustainable and welcome uses of a global resource, Un-habitat, 2009. ⟨https://unhabitat.org/global-atlas-of-excreta-wastewater-sludge-and-biosolids-management⟩.
[4] H. Rigby, A. Dowding, A. Fernandes, D. Humphries, N.R. Jones, I. Lake, R.G. Petch, C.K. Reynolds, M. Rose, S.R. Smith, Concentrations of organic contaminants in industrial and municipal bioresources recycled in agriculture in the UK, Sci. Total Environ. 765 (2021), 142787.
[5] Y. Yang, B. Meehan, K. Shah, A. Surapaneni, J. Hughes, L. Fouché, J. Paz-Ferreiro, Physicochemical properties of biochars produced from biosolids in Victoria, Australia, Int. J. Environ. Res. Public Health 15 (2018) 1459.
[6] Z. Liu, B.K. Mayer, K. Venkiteshwaran, S. Seyedi, A.S. Raju, D. Zitomer, P. J. McNamara, The state of technologies and research for energy recovery from municipal wastewater sludge and biosolids, Curr. Opin. Environ. Sci. 14 (2020) 31–36.
[7] A. Tomczyk, Z. Sokołowska, P. Boguta, Biochar physicochemical properties: pyrolysis temperature and feedstock kind effects, Rev. Environ. Sci. Biotechnol. 19 (2020) 191–215.
[8] A.C. Vilas-Boas, L.A. Tarelho, M. Kamali, T. Hauschild, D.T. Pio, D. Jahanianfard, A.P.D. Gomes, M.A. Matos, Biochar from slow pyrolysis of biological sludge from wastewater treatment: characteristics and effect as soil amendment, Biofuel Bioprod. Biorefin. 15 (2021) 1054–1072.
[9] S. Patel, S. Kundu, P. Halder, L. Rickards, J. Paz-Ferreiro, A. Surapaneni, S. Madapusi, K. Shah, Thermogravimetric analysis of biosolids pyrolysis in the presence of mineral oxides, Renew. Energy 141 (2019) 707–716.
[10] P. Cely, G. Gascó, J. Paz-Ferreiro, A. Méndez, Agronomic properties of biochars from different manure wastes, J. Anal. Appl. Pyrolysis 111 (2015) 173–182.
[11] A. Méndez, M. Terradillos, G. Gascó, Physicochemical and agronomic properties of biochar from sewage sludge pyrolysed at different temperatures, J. Anal. Appl. Pyrolysis 102 (2013) 124–130.
[12] E. Antunes, J. Schumann, G. Brodie, M.V. Jacob, P.A. Schneider, Biochar produced from biosolids using a single-mode microwave: Characterisation and its potential for phosphorus removal, J. Environ. Manag. 196 (2017) 119–126.
[13] C. Figueiredo, H. Lopes, T. Coser, A. Vale, J. Busato, N. Aguiar, E. Novotny, L. Canellas, Influence of pyrolysis temperature on chemical and physical properties of biochar from sewage sludge, Arch. Agron. Soil Sci. 64 (2018) 881–889.
[14] M.K. Hossain, V. Strezov, K.Y. Chan, A. Ziolkowski, P.F. Nelson, Influence of pyrolysis temperature on production and nutrient properties of wastewater sludge biochar, J. Environ. Manag. 92 (2011) 223–228.
[15] S. Patel, S. Kundu, P. Halder, G. Veluswamy, B. Pramanik, J. Paz-Ferreiro, A. Surapaneni, K. Shah, Slow pyrolysis of biosolids in a bubbling fluidised bed reactor using biochar, activated char and lime, J. Anal. Appl. Pyrolysis 144 (2019), 104697.
[16] S. Adhikari, G. Gascó, A. Méndez, A. Surapaneni, V. Jegatheesan, K. Shah, J. Paz-Ferreiro, Influence of pyrolysis parameters on phosphorus fractions of biosolids derived biochar, Sci. Total Environ. 695 (2019), 133846.
[17] S. Guo, X. Xiong, D. Che, H. Liu, B. Sun, Effects of sludge pyrolysis temperature and atmosphere on characteristics of biochar and gaseous products, Korean J. Chem. Eng. 38 (2021) 55–63.
[18] M. Kończak, P. Oleszczuk, K. Różyło, Application of different carrying gases and ratio between sewage sludge and willow for engineered (smart) biochar production, J. CO_2 Util. 29 (2019) 20–28.
[19] Z. Liu, F. Zhang, H. Liu, F. Ba, S. Yan, J. Hu, Pyrolysis/gasification of pine sawdust biomass briquettes under carbon dioxide atmosphere: Study on carbon dioxide reduction (utilization) and biochar briquettes physicochemical properties, Bioresour. Technol. 249 (2018) 983–991.
[20] C. Jindarom, V. Meeyoo, B. Kitiyanan, T. Rirksomboon, P. Rangsunvigit, Surface characterization and dye adsorptive capacities of char obtained from pyrolysis/gasification of sewage sludge, Chem. Eng. Sci. 133 (2007) 239–246.
[21] Q. Wang, K. Li, Z. Guo, M. Fang, Z. Luo, K. Cen, Effects of CO_2 atmosphere on slow pyrolysis of high-ash lignite, Carbon Resour. Convers. 1 (2018) 94–103.
[22] A.B. Hernández, F. Okonta, N. Freeman, Thermal decomposition of sewage sludge under N2, CO_2 and air: Gas characterization and kinetic analysis, J. Environ. Manag. 196 (2017) 560–568.
[23] J. Huang, J. Zhang, J. Liu, W. Xie, J. Kuo, K. Chang, M. Buyukada, F. Evrendilek, S. Sun, Thermal conversion behaviors and products of spent mushroom substrate in CO_2 and N2 atmospheres: kinetic, thermodynamic, TG and Py-GC/MS analyses, J. Anal. Appl. Pyrolysis 139 (2019) 177–186.
[24] M. Azuara, E. Sáiz, J.A. Manso, F.J. García-Ramos, J.J. Manyà, Study on the effects of using a carbon dioxide atmosphere on the properties of vine shoots-derived biochar, J. Anal. Appl. Pyrolysis 124 (2017) 719–725.
[25] M. Kończak, Y. Gao, P. Oleszczuk, Carbon dioxide as a carrier gas and biomass addition decrease the total and bioavailable polycyclic aromatic hydrocarbons in biochar produced from sewage sludge, Chemosphere 228 (2019) 26–34.
[26] M. Kończak, P. Oleszczuk, Co-pyrolysis of sewage sludge and biomass in carbon dioxide as a carrier gas affects the total and leachable metals in biochars, J. Hazard. Mater. 400 (2020), 123144.
[27] A.D. Igalavithana, X. Yang, H.R. Zahra, F.M. Tack, D.C. Tsang, E.E. Kwon, Y.S. Ok, Metal (loid) immobilization in soils with biochars pyrolyzed in N_2 and CO_2 environments, Sci. Total Environ. 630 (2018) 1103–1114.
[28] A.D. Igalavithana, K.-H. Kim, J.-M. Jung, H.-S. Heo, E.E. Kwon, F.M. Tack, D. C. Tsang, Y.J. Jeon, Y.S. Ok, Effect of biochars pyrolyzed in N_2 and CO_2, and feedstock on microbial community in metal (loid) s contaminated soils, Environ. Int. 126 (2019) 791–801.
[29] S. Farhangi-Abriz, S. Torabian, R. Qin, C. Noulas, Y. Lu, S. Gao, Biochar effects on yield of cereal and legume crops using meta-analysis, Sci. Total Environ. 775 (2021), 145869.
[30] S. Patel, S. Kundu, J. Paz-Ferreiro, A. Surapaneni, L. Fouche, P. Halder, A. Setiawan, K. Shah, Transformation of biosolids to biochar: a case study, Environ. Prog. Sustain. Energy 38 (2019) 13113.
[31] I. Benavente, G. Gasco, C. Plaza, J. Paz-Ferreiro, A. Mendez, Choice of pyrolysis parameters for urban wastes affects soil enzymes and plant germination in a Mediterranean soil, Sci. Total Environ. 634 (2018) 1308–1314.
[32] G. Pilon, J.-M. Lavoie, Pyrolysis of switchgrass (Panicum virgatum L.) at low temperatures within N_2 and CO_2 environments: Product yield study, ACS Sustain. Chem. Eng. 1 (2013) 198–204.
[33] C. Guizani, F.E. Sanz, S. Salvador, Effects of CO_2 on biomass fast pyrolysis: Reaction rate, gas yields and char reactive properties, Fuel 116 (2014) 310–320.
[34] J. Wang, S. Wang, Preparation, modification and environmental application of biochar: a review, J. Clean. Prod. 227 (2019) 1002–1022.
[35] T. Chen, Y. Zhang, H. Wang, W. Lu, Z. Zhou, Y. Zhang, L. Ren, Influence of pyrolysis temperature on characteristics and heavy metal adsorptive performance of biochar derived from municipal sewage sludge, Bioresour. Technol. 164 (2014) 47–54.
[36] K.B. Cantrell, P.G. Hunt, M. Uchimiya, J.M. Novak, K.S. Ro, Impact of pyrolysis temperature and manure source on physicochemical characteristics of biochar, Bioresour. Technol. 107 (2012) 419–428.
[37] W. Song, M. Guo, Quality variations of poultry litter biochar generated at different pyrolysis temperatures, J. Anal. Appl. Pyrolysis 94 (2012) 138–145.
[38] S.D. Joseph, M. Camps-Arbestain, Y. Lin, P. Munroe, C. Chia, J. Hook, L. Van Zwieten, S. Kimber, A. Cowie, B. Singh, An investigation into the reactions of biochar in soil, Soil Res. 48 (2010) 501–515.
[39] C. Banik, M. Lawrinenko, S. Bakshi, D.A. Laird, Impact of pyrolysis temperature and feedstock on surface charge and functional group chemistry of biochars, J. Environ. Qual. 47 (2018) 452–461.
[40] A. Shaaban, S.-M. Se, N.M.M. Mitan, M. Dimin, Characterization of biochar derived from rubber wood sawdust through slow pyrolysis on surface porosities and functional groups, Procedia Eng. 68 (2013) 365–371.
[41] E. Agrafioti, G. Bouras, D. Kalderis, E. Diamadopoulos, Biochar production by sewage sludge pyrolysis, J. Anal. Appl. Pyrolysis 101 (2013) 72–78.
[42] H. Lu, W. Zhang, Y. Yang, X. Huang, S. Wang, R. Qiu, Relative distribution of Pb2+ sorption mechanisms by sludge-derived biochar, Water Res. 46 (2012) 854–862.
[43] S. Li, S. Harris, A. Anandhi, G. Chen, Predicting biochar properties and functions based on feedstock and pyrolysis temperature: a review and data synthesis, J. Clean. Prod. 215 (2019) 890–902.
[44] Z. Fang, F. Liu, Y. Li, B. Li, T. Yang, R. Li, Influence of microwave-assisted pyrolysis parameters and additives on phosphorus speciation and transformation in phosphorus-enriched biochar derived from municipal sewage sludge, J. Clean. Prod. 287 (2021), 125550.
[45] C. Fang, T. Zhang, P. Li, Rf Jiang, Y.C. Wang, Application of magnesium modified corn biochar for phosphorus removal and recovery from swine wastewater, Int. J. Environ. 11 (2014) 9217–9237.
[46] Y. Chun, G. Sheng, C.T. Chiou, B. Xing, Compositions and sorptive properties of crop residue-derived chars, Sci. Total Environ. 38 (2004) 4649–4655.
[47] J. Wang, S. Wang, Preparation, modification and environmental application of biochar: a review, J. Clean. Prod. 227 (2021) 1002–1022.
[48] H. Lu, W. Zhang, S. Wang, L. Zhuang, Y. Yang, R. Qiu, Characterization of sewage sludge-derived biochars from different feedstocks and pyrolysis temperatures, J. Anal. Appl. Pyrolysis 102 (2013) 137–143.
[49] J. Jin, Y. Li, J. Zhang, S. Wu, Y. Cao, P. Liang, J. Zhang, M.H. Wong, M. Wang, S. Shan, Influence of pyrolysis temperature on properties and environmental safety of heavy metals in biochars derived from municipal sewage sludge, J. Hazard. Mater. 320 (2016) 417–426.
[50] O. Francioso, M.T. Rodriguez-Estrada, D. Montecchio, C. Salomoni, A. Caputo, D. Palenzona, Chemical characterization of municipal wastewater sludges

produced by two-phase anaerobic digestion for biogas production, J. Hazard. Mater. 175 (2010) 740–746.
[51] Q. Chang, R. Gao, H. Li, Z. Dai, G. Yu, X. Liu, F. Wang, Effects of CO_2 on coal rapid pyrolysis behavior and chemical structure evolution, J. Anal. Appl. Pyrolysis 128 (2017) 370–378.
[52] X. Chen, S. Jeyaseelan, N. Graham, Physical and chemical properties study of the activated carbon made from sewage sludge, Waste Manag. 22 (2002) 755–760.
[53] Y. Bai, P. Wang, L. Yan, C. Liu, F. Li, K. Xie, Effects of CO_2 on gas evolution and char structure formation during lump coal pyrolysis at elevated pressures, J. Anal. Appl. Pyrolysis 104 (2013) 202–209.
[54] H. Jin, R.O. Arazo, J. Gao, S. Capareda, Z. Chang, Leaching of heavy metals from fast pyrolysis residues produced from different particle sizes of sewage sludge, J. Anal. Appl. Pyrolysis 109 (2014) 168–175.
[55] H.J. Huang, T. Yang, F.-Y. Lai, G.-Q. Wu, Co-pyrolysis of sewage sludge and sawdust/rice straw for the production of biochar, J. Anal. Appl. Pyrolysis 125 (2017) 61–68.
[56] A. Zielińska, P. Oleszczuk, B. Charmas, J. Skubiszewska-Zięba, S. Pasieczna-Patkowska, Effect of sewage sludge properties on the biochar characteristic, J. Anal. Appl. Pyrolysis 112 (2015) 201–213.
[57] X. Peng, L. Ye, C. Wang, H. Zhou, B. Sun, Temperature-and duration-dependent rice straw-derived biochar: Characteristics and its effects on soil properties of an Ultisol in southern China, Soil Tillage Res. 112 (2011) 159–166.
[58] C. Jindarom, V. Meeyoo, T. Rirksomboon, P. Rangsunvigit, Thermochemical decomposition of sewage sludge in CO_2 and N_2 atmosphere, Chemosphere 67 (2007) 1477–1484.
[59] A. Downie, A. Crosky, P. Munroe, Physical propierties of biochar, in: J. Lehmann, S. Joseph (Eds.), Biochar for Environmental Management: Science and Technology, Earthscan Ltd, London, 2015.
[60] H. Yuan, T. Lu, H. Huang, D. Zhao, N. Kobayashi, Y. Chen, Influence of pyrolysis temperature on physical and chemical properties of biochar made from sewage sludge, J. Anal. Appl. Pyrolysis 112 (2015) 284–289.
[61] L. Liu, L. Huang, R. Huang, H. Lin, D. Wang, Immobilization of heavy metals in biochar derived from co-pyrolysis of sewage sludge and calcium sulfate, J. Hazard. Mater. 403 (2021), 1236483648.
[62] S. Ramola, T. Belwal, C.J. Li, Y.Y. Wang, H.H. Lu, S.M. Yang, C.H. Zhou, Improved lead removal from aqueous solution using novel porous bentonite-and calcite-biochar composite, Sci. Total Environ. 709 (2020), 136171.
[63] K. Crombie, O. Mašek, A. Cross, S. Sohi, Biochar–synergies and trade-offs between soil enhancing properties and C sequestration potential, Glob. Change Biol. 7 (2015) 1161–1175.
[64] X. Liu, A. Zhang, C. Ji, S. Joseph, R. Bian, L. Li, G. Pan, J. Paz-Ferreiro, Biochar's effect on crop productivity and the dependence on experimental conditions—a meta-analysis of literature data, Plant Soil 373 (2013) 583–594.
[65] M. Kończak, B. Pan, Y.S. Ok, P. Oleszczuk, Carbon dioxide as a carrier gas and mixed feedstock pyrolysis decreased toxicity of sewage sludge biochar, Sci. Total Environ. 723 (2020), 137796.